Improved molecular structure retrieval method for photoelectron holography

Chengjian Yu and Xu Wang*
Graduate School, China Academy of Engineering Physics, Beijing 100193, China

(Received 29 August 2019; revised manuscript received 14 November 2019; published 20 December 2019)

Photoelectron holography is a method that retrieves molecular structure information from photoelectron diffraction patterns generated by x-ray free-electron lasers, which have the promise of following dynamic molecular structure evolutions with angstrom spatial and femtosecond temporal resolutions (the so-called molecular movie). However, an additional phase is introduced when the photoelectron is scattered by an atom, and this scattering phase turns into a spatial error when the position of the atom is retrieved using a Fourier-type transform. We propose a method to remove, or greatly suppress, this error, with demonstrations using numerical examples.

DOI: 10.1103/PhysRevA.100.063422

I. INTRODUCTION

The development of x-ray free-electron lasers (XFELs) delivers the promise of imaging dynamic molecular structure evolutions with angstrom spatial and femtosecond temporal resolutions [1–5]. Dynamic structure evolutions of isolated (gas-phase) molecules provide the most direct information about chemical reactions.

With the (expensive) XFEL light source available, how to fully utilize it for the above-mentioned goal of molecular structure imaging deserves extensive research efforts. Indeed, several proposals or demonstrations have been made [6]. Using elastic scattering of the x-ray photons, it has been demonstrated that the brilliant and ultrafast x-ray source can be used to image the structures of single biological molecules [7,8], nanocrystals [9], liquid droplets [10], gas-phase molecules [11], etc.

Another method uses photoelectron scattering [12–22] instead of photon scattering. An x-ray photon first pulls out an electron from an inner orbital localized at some chosen atom and, on its way out, the photoelectron is scattered by the surrounding atoms. Molecular structure information is therefore encoded in the photoelectron diffraction pattern. The diffraction pattern can be understood as the result of the interference between the direct wave, which goes directly from the emitter atom to the detector, and the scattered wave, which is scattered by nearby atoms before being detected. Similar in idea to optical holography [23], this method is also called photoelectron holography [12].

Converting an x-ray photon into a photoelectron gives the following advantages: First, a lower x-ray energy is needed to achieve the same de Broglie wavelength, which largely determines the spatial resolution. For instance, to reach the same de Broglie wavelength of 1 Å, a photon needs to have energy 12 keV, whereas an electron only needs to have energy 150 eV. The total photon energy needed in photoelectron diffraction is thus 150 eV plus the ionization potential of the photoelectron, which is usually much smaller than 12 keV. Second, electron diffraction is usually more favorable because the cross section of electron diffraction is about six orders of magnitude higher than that of x-ray photon diffraction.

The disadvantage of the photoelectron scattering method is that the interference pattern cannot be physically separated from the stronger background of the direct wave. Although the direct-wave background has simple smooth forms (such as a $\cos^2\theta$ angular dependency for a p wave) and can be subtracted, the data noise level needs to be low in order not to bury the interference pattern. Nevertheless, experiments have been performed with various gas-phase molecules, such as C_8H_5F [15], $C_6H_4Br_2$ [16], I_2 [17,19], CO_2 [21], CH_3I [22], etc.

Given a photoelectron diffraction pattern, there are mainly two ways to retrieve the structure of the molecule. The first way is fitting: adjusting the structural parameters of the molecule until the calculated diffraction pattern agrees with the experimental one [13,18–20]. The disadvantage is that the parameter space is usually multidimensional so the fitting process is time consuming. Besides, the fitting can easily be stuck in a local minimum instead of the global minimum, and the number of local minima is large for a multidimensional parameter space. *A priori* information about the structure is usually needed to limit the size of the parameter space.

The second way of retrieving a molecular structure from a diffraction pattern is direct inversion using Fourier-type transform, such as a Helmholtz-Kirchhoff (HK) transform [12,14]. This method is attractive in that no *a priori* knowledge about the molecular structure is required, and that the computational load is much smaller than multiparameter fitting. The disadvantage, as has been realized in practice [14] and will be more clearly explained in this paper, is that the retrieved atomic positions may have errors as large as 0.5 to 1.0 Å. This error is due to the additional phase introduced in electron-atom scattering. After performing HK transform, this scattering phase turns into a spatial error in the retrieved atomic position.

The goal of the current paper is to propose a method to remove, or at least greatly suppress, this retrieval error. Our idea is to divide from the diffraction pattern a theoretical

*xwang@gscaep.ac.cn

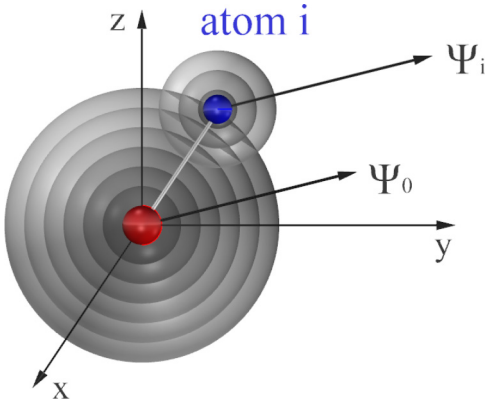

FIG. 1. Illustration of photoelectron holography. A photoelectron is pulled out by an x-ray pulse from a chosen atom and going out as a spherical wave. It can either go directly to the detector or be scattered by a surrounding atom i before being detected. Molecular structure information is encoded in the detected signal, which is the result of interference between the direct wave (Ψ_0) and the scattered wave (Ψ_i).

(complex) scattering factor before performing HK transform. The problematic scattering phase is thus removed. Numerical examples will be given, demonstrating that the retrieval error can indeed be largely suppressed.

This paper is organized as follows. In Sec. II, we first give a brief introduction to the photoelectron holography method and explain why the electron scattering phase is a problem leading to a retrieval error in atomic position. Then we propose a method to remove this error. Numerical testings and demonstrations will be given in Sec. III. A conclusion will be given in Sec. IV.

II. METHOD

A. Photoelectron holography: A brief introduction

Here we give a brief introduction to the method of photoelectron holography using a simple model. More details about the method can be found in earlier publications [12,18].

Assume the x-ray light (linearly polarized along the z direction) pulls out an electron from an inner orbital localized at some target atom, as illustrated in Fig. 1. (If the orbital is an s orbital, then the photoelectron will be a p wave along the polarization direction.) The photoelectron can either go directly to the detector [position $\vec{r} = (r, \theta, \phi)$] or be scattered by a surrounding atom [position $\vec{R}_i = (R_i, \theta_i, \phi_i)$] before being detected. The signal at the detector is

$$I(\vec{r}) = |\Psi_0(\vec{r}) + \Psi_i(\vec{r})|^2, \tag{1}$$

where Ψ_0 is the direct wave and Ψ_i is the wave scattered by atom i. Extension to the situation of more scattering atoms is straightforward. Note that by writing Eq. (1), we have neglected higher-order scatterings, i.e., the photoelectron being scattered more than once before arriving at the detector. This is usually a good approximation for photoelectron energies above about 100 eV [24].

The direct wave is assumed to be a p wave with the following form:

$$\Psi_0(\vec{r}) \propto \frac{e^{ikr}}{r}\cos\theta, \tag{2}$$

and the scattered wave Ψ_i can be written as

$$\Psi_i(\vec{r}) = \Psi_0(\vec{R}_i) f_i(\Theta) \frac{e^{ik|\vec{r}-\vec{R}_i|}}{|\vec{r}-\vec{R}_i|}. \tag{3}$$

The first factor on the right-hand side is the amplitude of the direct wave at position $\vec{R}_i$. The second factor is the electron scattering factor, which is in general complex and tells how much the incoming wave is modified in amplitude and in phase by the scattering atom. Note that the scattering factor is a function of the scattering angle Θ, which is the angle of diffraction with respect to the direction of the incoming wave. The third factor tells that a new spherical wave is emitted from the scattering atom.

Substituting Eqs. (2) and (3) into Eq. (1), we get

$$\begin{aligned} I(\vec{r}) &\propto \left| \frac{e^{ikr}}{r}\cos\theta + \frac{e^{ikR_i}}{R_i}\cos\theta_i f_i(\Theta) \frac{e^{ik|\vec{r}-\vec{R}_i|}}{|\vec{r}-\vec{R}_i|} \right|^2 \\ &\approx \left| \frac{e^{ikr}}{r}\cos\theta + \frac{e^{ikR_i}}{R_i}\cos\theta_i f_i(\Theta) \frac{e^{ikr}}{r} e^{-i\vec{k}\cdot\vec{R}_i} \right|^2 \\ &= \frac{1}{r^2}\left| \cos\theta + \frac{e^{ikR_i}}{R_i}\cos\theta_i f_i(\Theta) e^{-i\vec{k}\cdot\vec{R}_i} \right|^2. \end{aligned} \tag{4}$$

From the first to the second step, we have used the approximation that for large r, $e^{ik|\vec{r}-\vec{R}_i|}/|\vec{r}-\vec{R}_i| \approx (e^{ikr}/r)e^{-i\vec{k}\cdot\vec{R}_i}$. Because the absolute signal value has no significance, we can neglect the $1/r^2$ term and get

$$I(\theta, \phi) \propto \left| \cos\theta + \frac{e^{ikR_i}}{R_i}\cos\theta_i f_i(\Theta) e^{-i\vec{k}\cdot\vec{R}_i} \right|^2 \tag{5}$$

$$\equiv I_0(\theta) + I_1(\theta, \phi) + I_2(\theta, \phi). \tag{6}$$

Note that the scattering angle $\Theta = \Theta(\theta, \phi)$. I_0, I_1, I_2 are given as follows:

$$I_0(\theta) = \cos^2\theta, \tag{7}$$

$$I_1(\theta, \phi) = \cos\theta\cos\theta_i f_i(\Theta) \frac{e^{ikR_i}}{R_i} e^{-i\vec{k}\cdot\vec{R}_i} + \text{c.c.}, \tag{8}$$

$$I_2(\theta, \phi) = \frac{1}{R_i^2}\cos^2\theta_i |f_i(\Theta)|^2. \tag{9}$$

Molecular structure information is mainly coded in I_1. Among the three parts, I_0 is the major part of the signal of photoelectron, and I_1 is normally stronger than I_2.

I_0 contains no structural information, but it can be removed from the signal due to its simple form. Krasniqi *et al.* [12] borrow the HK transform from optical holography and propose to transform $(I - I_0)$,

$$U(\vec{x}) = \iint (I - I_0) e^{i\vec{k}\cdot\vec{x}} \sin\theta d\theta d\phi. \tag{10}$$

This can be understood as a special type of Fourier transform: Only the angles of $\vec{k}$ are integrated out, and the length of $\vec{k}$ is fixed (due to fixed photon energy).

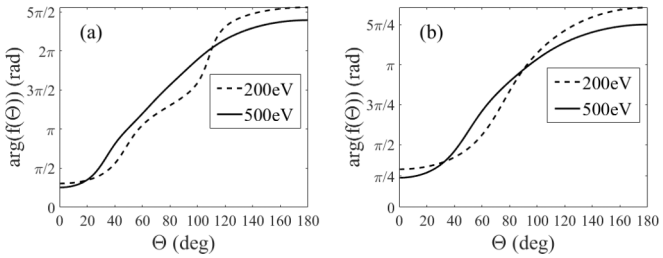

FIG. 2. Electron scattering phases for (a) the Cl atom and (b) the F atom at two different scattering energies, obtained using the code ELSEPA and a muffin-tin radius of 1.63 a.u. for Cl and 1.16 a.u. for F.

B. The scattering phase problem

To have a better understanding of the HK transform of Eq. (10), let us neglect I_2, which is normally weaker than I_1. Then, $I - I_0 \approx I_1$. With Eq. (8), we get

$$U(\vec{x}) = \cos\theta_i \frac{e^{ikR_i}}{R_i} \iint \cos\theta f_i(\Theta) e^{i\vec{k}\cdot(\vec{x}-\vec{R}_i)} \sin\theta d\theta d\phi + \cos\theta_i \frac{e^{-ikR_i}}{R_i} \iint \cos\theta f_i^*(\Theta) e^{i\vec{k}\cdot(\vec{x}+\vec{R}_i)} \sin\theta d\theta d\phi. \tag{11}$$

If the phase of f_i can be neglected, as in photon scattering, then $U(\vec{x})$ peaks at $\vec{x} = \pm\vec{R}_i$. So the correct position of atom i is retrieved, together with its twin image. (The $\cos\theta$ term, as a result of the p wave, will cause another subtlety, which will be explained later in Sec. III.)

However, in electron scattering, the phase of f_i may not be neglected. For example, Fig. 2 shows the electron scattering phase for the Cl atom and for the F atom at two different scattering energies (200 and 500 eV), obtained using the code ELSEPA [25], which performs Dirac partial-wave calculations of elastic scattering of electrons by atoms or positive ions. A muffin-tin radius of 1.63 a.u. is assigned to Cl and 1.16 a.u. for F, using a touching-sphere technique [18]. The phase depends sensitively on and increases with the scattering angle. For 180°, the scattering phase can be as large as 2.5π for Cl and 1.5π for F.

As can be seen from Eq. (11), the scattering phase turns into an error in the retrieved atomic position. If we use 1.5π as an estimation of the scattering phase, it will lead to a retrieval error of $1.5\pi/k = 0.77$ a.u. for 500 eV, and 1.24 a.u. for 200 eV. These are sizable errors for small or medium molecules.

C. A proposal to solve the scattering phase problem

We propose to solve the above explained scattering phase problem by dividing a theoretical scattering factor before performing the HK transform,

$$U_{\text{new}}(\vec{x}) = \iint \frac{I - I_0}{f_i^{\text{th}}(\Theta)} e^{i\vec{k}\cdot\vec{x}} \sin\theta d\theta d\phi, \tag{12}$$

where $f_i^{\text{th}}(\Theta)$ is a theoretically calculated electron scattering factor for atom i. By doing so, the retrieval error from the electron scattering phase can largely be suppressed. This will be confirmed by our numerical results presented in the following section. We noticed that a similar method was proposed by Tonner *et al.* for metal (Cu) thin films [26]. This paper will be focused on a gas-phase molecule (CF_3Cl), with the complication that the scattering pattern is the result of different kinds of scattering atoms, in contrast to a metal thin film composed of a single kind of atom.

The theoretical scattering factor $f_i^{\text{th}}(\Theta)$ is obtained using the code ELSEPA. A muffin-tin radius is used as an input parameter of the code, and the radius is determined by a touching-sphere technique [18,19]. Our experience was that the scattering phase is not very sensitive to the muffin-tin radius, but the scattering amplitude $|f(\Theta)|$ for small scattering angles (i.e., forward scattering) is sensitive to the muffin-tin radius.

To implement $f_i^{\text{th}}(\Theta)$ into Eq. (12), we need to know the spatial orientation of atom i. However, that is the unknown information that we wanted to obtain from the retrieval. We use the following two-step procedure for the retrieval: First, we perform the original HK transform as shown in Eq. (10) to get a rough position for each atom; second, with the rough position of each atom, we perform the improved HK transform as shown in Eq. (12) to get a more precise position for each atom. That is, Eq. (12) needs to be calculated for each atom separately.

Implicit in writing Eq. (12) is the single-scattering approximation, valid with relatively high photoelectron energies (above about 100 eV). With the single-scattering approximation, the scattering wave from each individual atom interferes independently with the direct wave. So atoms are independent, allowing a separate application of Eq. (12) to each atom.

III. NUMERICAL RESULTS AND DISCUSSIONS

A. HK transform vs improved HK transform

We use the molecule CF_3Cl to demonstrate the method that we proposed in the previous section. The structure of this molecule is illustrated in Fig. 3(a). The C atom is in the center and set to be the origin of the coordinate. The Cl atom is on the $+z$ axis, and the three F atoms are below the C atom. The experimental equilibrium Cl-C bond length is 3.31 a.u. and the C-F bond length is 2.50 a.u. The Cl-C-F bond angle is 110.3°. The orientation of the three F atoms is such that one of the F atoms is in the x-z plane.

Two example photoelectron diffraction patterns are given in Figs. 3(b) and 3(c). The photoelectron is assumed to be pulled out from the 1s orbital of the C atom by an x-ray laser linearly polarized along the z axis [Fig. 3(b)] and the x axis [Fig. 3(c)]. The energy of the photoelectron is assumed to be 500 eV in both cases. The configuration used in Fig. 3(b) is better for retrieving the position of the Cl atom, while the configuration used in Fig. 3(c) is better for retrieving the position of the F atom located in the x-z plane, due to the spatial orientation of the emitted p wave. These photoelectron diffraction patterns are obtained using the single-scattering model explained in Sec. II A. Next we use Figs. 3(b) and 3(c) to perform the HK transform of Eq. (10) and the improved HK transform of Eq. (12). The transform is performed for each three-dimensional (3D) vector $\vec{x}$. For ease of presentation, we only show $|U(\vec{x})|$ and $|U_{\text{new}}(\vec{x})|$ on the x-z plane. Because the

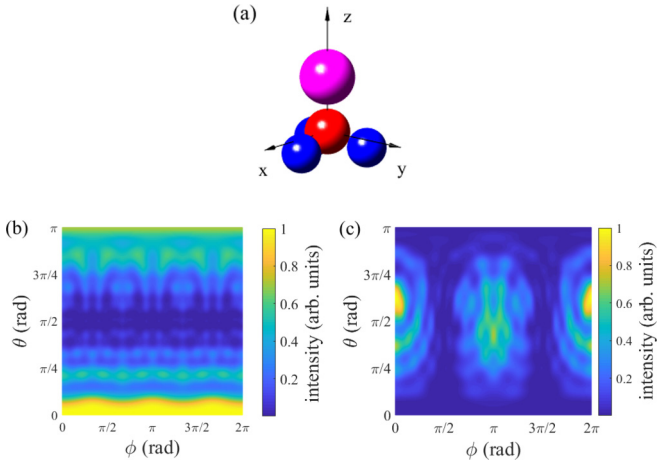

FIG. 3. (a) Illustration of the CF_3Cl molecule. The Cl atom is at the top, the C atom is in the center, set as the origin of the coordinate, and the F atoms are below the C atom. One of the F atoms is in the x-z plane. (b) An example photoelectron diffraction pattern. The photoelectron is assumed to be pulled out from the $1s$ orbital of the C atom, by an x-ray pulse linearly polarized along the z axis. The energy of the electron is 500 eV. (c) Photoelectron diffraction pattern if the x-ray pulse is polarized along the x axis. Other parameters are the same as (b).

Cl atom and one of the F atoms are in the x-z plane, it is adequate for our purpose of demonstration.

Let us first focus on the upper x-z plane. The diffraction pattern used is shown in Fig. 3(b). Figure 4 shows $|U(\vec{x})|$ [Fig. 4(a)] and $|U_{\rm new}(\vec{x})|$ [Fig. 4(b)] for the upper x-z plane. The black cross on each panel marks the actual position ($x = 0$, $z = 3.31$ a.u.) of the Cl atom. The original HK transform shown in Fig. 4(a) gives a brightest spot, which is taken as the retrieved position of the Cl atom, at ($x = 0$, $z = 4.23$ a.u.). The error is 0.92 a.u., or 28% relative to the correct value.

Figure 4(b) shows $|U_{\rm new}(\vec{x})|$ using the improved HK transform. Instead of giving a single outstanding bright spot, the improved HK transform usually gives two (almost) equally bright spots. The correct retrieval position of the atom should be taken at the node between the two bright spots. This is a consequence of the p wave from the $\cos\theta$ term, and requires a little more explanation. Let us go back to Eq. (11) and take a closer look at the first line. Suppose $f_i(\Theta)$ has been completely counteracted by a theoretical $f_i^{\rm th}(\Theta)$, and also $\vec{x}$=$\vec{R}_i$;

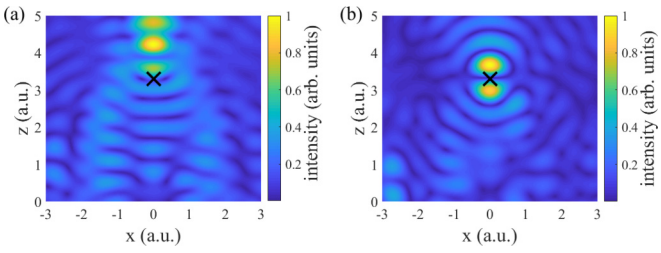

FIG. 4. (a) $|U(\vec{x})|$ from the original HK transform and $|U_{\rm new}(\vec{x})|$ from the improved HK transform. The black cross on each panel marks the correct position of the Cl atom.

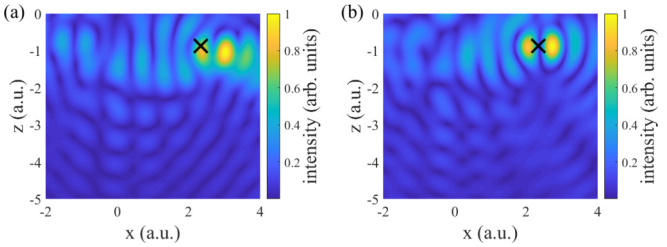

FIG. 5. Same as Fig. 4, but for the F atom in the lower x-z plane.

then we are still left with the integral $\int_0^\pi \cos\theta \sin\theta d\theta = 0$. Without this $\cos\theta$ term, we are expecting a single bright spot at $\vec{x} = \vec{R}_i$. The $\cos\theta$ term cuts the bright spot in half (later, in Sec. III C, we will show that the node is gone for circular polarization when we replace $\cos\theta$ with $\sin\theta$). And it is actually the node between the two bright spots that should be taken as the retrieved position of the atom. One sees from Fig. 4(b) that the node between the two bright spots is almost identical to the correct position of the Cl atom. The improved HK transform can indeed remove the error due to the electron-atom scattering phase.

Next let us move to the lower x-z plane. The diffraction pattern used is shown in Fig. 3(c). Figure 5(a) shows $|U(\vec{x})|$ from the original HK transform. The correct position is ($x = 2.35$ a.u., $z = -0.867$ a.u.), corresponding to a C-F bond length of 2.5 a.u. The brightest spot in the $|U(\vec{x})|$ from the original HK transform is $x = 3.04$ a.u., $z = -1.05$ a.u., corresponding to a C-F bond length of 3.22 a.u., a 28% error to the correct value. Figure 5(b) shows $|U_{\rm new}(\vec{x})|$ from the improved HK transform, which uses the scattering factor for the F atom. Again, similarly to the Cl atom case, two almost equally bright spots are obtained, and the node between the two is very close to the correct position of the F atom.

B. Diffraction pattern from EPOLYSCAT

In the above results, we have used the same scattering factors $f_i(\Theta)$ (i = Cl, F) to generate the diffraction pattern and to perform the improved HK transform. The discrepancies shown in Figs. 4(a) and 5(a) from the original HK transform are therefore purely due to the scattering phase. And we have demonstrated that by using the improved HK transform, we indeed can remove the scattering phase error and obtain the desired atomic position.

We show that our method remains valid even though the theoretical scattering factor $f_i^{\rm th}(\Theta)$ is not quite the same as the real scattering factor. Now we start our retrieval from a photoelectron diffraction pattern generated from the EPOLYSCAT code [27,28], which iteratively solves the Schwinger equation. The diffraction pattern by EPOLYSCAT includes contributions from multiple-scattering processes and does not use any external electron-atom scattering factor. The obtained $|U(\vec{x})|$ from the original HK transform and the $|U_{\rm new}(\vec{x})|$ from the improved HK transform are shown in Figs. 6(a) and 6(b), respectively, to be compared with Fig. 4. One sees that the original HK transform still leads to a sizable error to the position of the Cl atom, and that the error can largely be removed by using the improved HK transform as proposed.

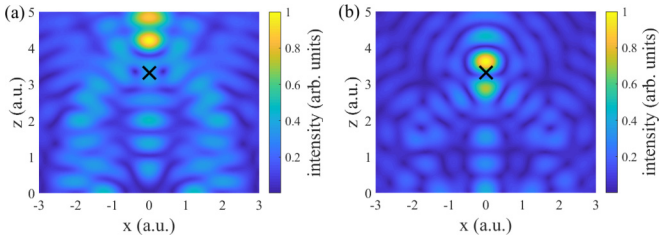

FIG. 6. Same as Fig. 4, but starting with the photoelectron diffraction pattern generated from the EPOLYSCAT code.

C. Circularly polarized x rays

In this section, we show that our method also applies to circular polarization (CP), provided a slight modification is made to compensate an additional phase initiated by CP. Assume an electron is pulled out by a circularly polarized x-ray light (by convention, the z axis is now the propagation axis) from an s orbital and the emitted electron wave has the following form:

$$\Psi_0(\vec{r}) \propto \frac{e^{ikr}}{r} \sin\theta e^{i\phi}. \tag{13}$$

The diffraction pattern becomes [to be compared with Eq. (5) for linear polarization]

$$I(\theta,\phi) \propto \left| \sin\theta e^{i\phi} + \frac{e^{ikR_i}}{R_i} \sin\theta_i e^{i\phi_i} f_i(\Theta) e^{-i\vec{k}\cdot\vec{R}_i} \right|^2, \tag{14}$$

where $\{R_i, \theta_i, \phi_i\}$ is the position of atom i. The interference term becomes

$$I_1(\theta,\phi) = \sin\theta e^{-i\phi} \sin\theta_i e^{i\phi_i} f_i(\Theta) \frac{e^{ikR_i}}{R_i} e^{-i\vec{k}\cdot\vec{R}_i} + \text{c.c.} \tag{15}$$

One sees that both the phase of $f_i(\Theta)$ and the phase $e^{-i\phi}$ become sources of error in the retrieval. We only need to modify Eq. (12) slightly to compensate the CP-induced phase,

$$U_{\text{CP}}(\vec{x}) = \iint \frac{I - I_0}{f_i^{\text{th}}(\Theta)} e^{i\phi} e^{i\vec{k}\cdot\vec{x}} \sin\theta d\theta d\phi. \tag{16}$$

Figure 7(a) shows an example photoelectron diffraction pattern for CP with the same molecule as used above. The energy of the photoelectron is also 500 eV. The retrieved position of the F atom in the lower x-z plane is shown in Fig. 7(b), using the original HK transform [Eq. (10)], and in Fig. 7(c), using the improved HK transform for CP [Eq. (16)]. One sees that the improved HK transform yields the desired position of the atom. Besides, the node structure shown in linear polarization due to the $\cos\theta$ term no longer exists for circular polarization, and a single bright spot is seen.

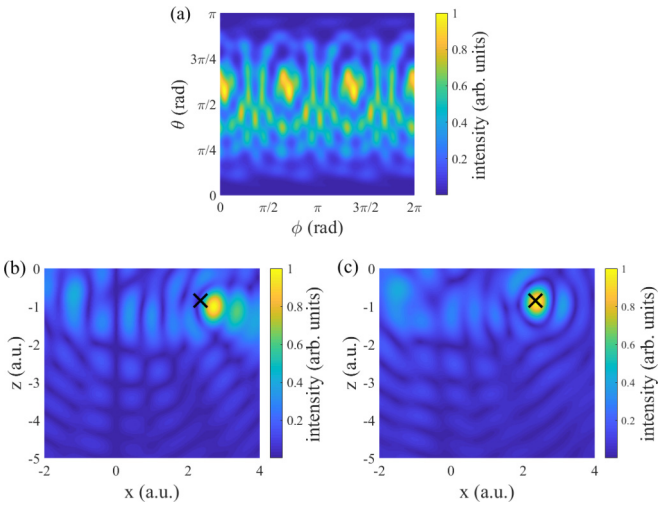

FIG. 7. (a) Photoelectron diffraction pattern of CF_3Cl by a circularly polarized x-ray. The energy of the electron is 500 eV. (b),(c) Retrieved position of the F atom in the lower x-z plane from the original HK transform [Eq. (10)] and from the improved HK transform for CP [Eq. (16)]. The black cross marks the correct position of the atom.

IV. CONCLUSION

In this paper, we discuss one aspect of the photoelectron holography method, which is used to retrieve molecular structure information from photoelectron diffraction patterns. The concept of photoelectron holography is in analogy to optical holography. However, unlike negligible photon-atom scattering phases, electron-atom scattering phases are usually too large to be simply neglected. These scattering phases turn into spatial errors when the atomic positions are retrieved using the Helmholtz-Kirchhoff transform. We have proposed a simple method to remove (or greatly suppress) these errors, by dividing from the diffraction pattern theoretically calculated electron scattering factors before performing the HK transform. Our proposed method has been demonstrated and verified by numerical examples, with both linearly polarized and circularly polarized x rays.

ACKNOWLEDGMENTS

We acknowledge support from the National Science Foundation of China Grant No. 11774323, Science Challenge Project of China Grant No. TZ2018005, National Key R&D Program of China Grant No. 2017YFA0403200, and NSAF Grant No. U1730449.

[1] B. W. J. McNeil and N. R. Thompson, Nat. Photon. **4**, 814 (2010).
[2] P. Bucksbaum and N. Berrah, Phys. Today **68**(7), 26 (2015).
[3] A. Fratalocchi and G. Ruocco, Phys. Rev. Lett. **106**, 105504 (2011).
[4] K. J. Gaffney and H. N. Chapman, Science **316**, 1444 (2007).
[5] M. P. Minitti, J. M. Budarz, A. Kirrander, J. S. Robinson, D. Ratner, T. J. Lane, D. Zhu, J. M. Glownia, M. Kozina, H. T. Lemke *et al.*, Phys. Rev. Lett. **114**, 255501 (2015).
[6] J. Miao, T. Ishikawa, I. K. Robinson, and M. M. Murnane, Science **348**, 530 (2015).
[7] M. M. Seibert *et al.*, Nature (London) **470**, 78 (2011).
[8] H. N. Chapman *et al.*, Nat. Mater. **8**, 299 (2009).

[9] H. N. Chapman *et al.*, Nature (London) **470**, 73 (2011).
[10] L. F. Gomez *et al.*, Science **345**, 906 (2014).
[11] J. Küpper *et al.*, Phys. Rev. Lett. **112**, 083002 (2014).
[12] F. Krasniqi, B. Najjari, L. Strüder, D. Rolles, A. Voitkiv, and J. Ullrich, Phys. Rev. A **81**, 033411 (2010).
[13] M. Kazama, T. Fujikawa, N. Kishimoto, T. Mizuno, J. I. Adachi, and A. Yagishita, Phys. Rev. A **87**, 063417 (2013).
[14] S. X.-L. Sun, A. P. Kaduwela, A. X. Gray, and C. S. Fadley, Phys. Rev. A **89**, 053415 (2014).
[15] R. Boll, D. Anielski, C. Bostedt, J. D. Bozek, L. Christensen, R. Coffee, S. De, P. Decleva, S. W. Epp, B. Erk, L. Foucar, F. Krasniqi, J. Kupper, A. Rouzee, B. Rudek, A. Rudenko, S. Schorb, H. Stapelfeldt, M. Stener, S. Stern, S. Techert, S. Trippel, M. J. J. Vrakking, J. Ullrich, and D. Rolles, Phys. Rev. A **88**, 061402(R) (2013).
[16] D. Rolles *et al.*, J. Phys. B **47**, 124035 (2014).
[17] K. Nakajima *et al.*, Sci. Rep. **5**, 14065 (2015).
[18] X. Wang, A.-T. Le, C. Yu, R. R. Lucchese, and C. D. Lin, Sci. Rep. **6**, 23655 (2016).
[19] S. Minemoto *et al.*, Sci. Rep. **6**, 38654 (2016).
[20] S. Tsuru, T. Sako, T. Fujikawa, and A. Yagishita, Phys. Rev. A **95**, 043404 (2017).
[21] S. Tsuru, T. Sako, T. Fujikawa, and A. Yagishita, J. Chem. Phys. **150**, 174306 (2019).
[22] S. Tsuru, T. Sako, T. Fujikawa, and A. Yagishita, J. Chem. Phys. **151**, 104302 (2019).
[23] M. Born and E. Wolf, *Principles of Optics*, 7th ed. (Cambridge University Press, Cambridge, 1999), Chap. 8.10.
[24] J. Xu, Z. Chen, A. T. Le, and C. D. Lin, Phys. Rev. A **82**, 033403 (2010).
[25] F. Salvat, A. Jablonski, and C. J. Powell, Comput. Phys. Commun. **165**, 157 (2005).
[26] B. P. Tonner, Z. L. Han, G. R. Harp, and D. K. Saldin, Phys. Rev. B **43**, 14423 (1991).
[27] F. A. Gianturco, R. R. Lucchese, and N. Sanna, J. Chem. Phys. **100**, 6464 (1994).
[28] A. P. P. Natalense and R. R. Lucchese, J. Chem. Phys. **111**, 5344 (1999).